Inorganic Chemistry

Article

pubs.acs.org/IC

Undecaphenylcorroles

Steffen Berg,[†] Kolle E. Thomas,[†] Christine M. Beavers,[‡] and Abhik Ghosh*[,†]

[†]Department of Chemistry and Center for Theoretical and Computational Chemistry, University of Tromsø, 9037 Tromsø, Norway

[‡]Advanced Light Source (ALS), Lawrence Berkeley National Laboratory (LBNL), Berkeley, California 94720-8229, United States

Supporting Information

ABSTRACT: A first major study of undecaphenylcorrole (UPC) derivatives is presented. Three different Cu-UPC derivatives with different para substituents X (X = CF_3, H, CH_3) on the β-aryl groups were synthesized via Suzuki−Miyaura coupling of Cu[Br_8TPC] and the appropriate arylboronic acid. A single-crystal X-ray structure of the X = CF_3 complex revealed a distinctly saddled macrocycle conformation with adjacent pyrrole rings tilted by ∼60−66° relative to one another (within the dipyrromethane units), which is somewhat higher than that observed for β-unsubstituted Cu-TPC derivatives but slightly lower than that observed for Cu[Br_8TPC] (∼70°) derivatives. Electrochemical and electronic absorption measurements afforded some of the first comparative insights into meso versus β substituent effects on the copper corrole core. The Soret maxima of the Cu-UPC complexes (∼440−445 nm), however, are comparable to those of Cu[Br_8TPC] derivatives and are considerably red-shifted relative to Cu-TPC derivatives. Para substituents on the β-phenyl groups were found to tune the redox potentials of copper corroles more effectively than those on *meso*-phenyl substituents, a somewhat surprising observation given that neither the HOMO nor LUMO has significant amplitudes at the β-pyrrolic positions.

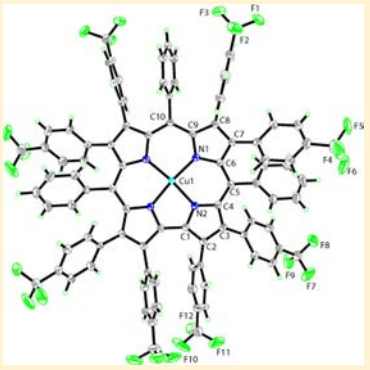

INTRODUCTION

Like their porphyrin counterparts,[1,2] sterically hindered corroles such as undecaphenylcorrole (UPC) derivatives (Figure 1) are of interest for many reasons. They offer, for example, the potential for shape-selective catalysis.[3] They also promise novel coordination complexes, which might be too unstable in the absence of a sterically protective ligand environment. The sterically hindered ligands should effectively preclude the formation of metal−metal-bonded dimers, a common occurrence with second- and third-row transition metals.[4,5] A third and crucial motivation for this study is that corroles, as trianionic ligands, support fundamentally different transition-metal chemistry, including different coordination, oxidation, and spin states, relative to the dianionic porphyrins.[6] These considerations led us to initiate a systematic study of UPC derivatives. Except for an isolated report on copper undecakis(*p*-chlorophenyl)corrole,[7] these fascinating ligands and their complexes remain virtually unexplored. We present here Suzuki−Miyaura[8] coupling-based syntheses of three Cu-UPC derivatives with varying *p*-X-substituted (X = CF_3, H, CH_3; Figure 2) β-aryl groups, Cu[(4-XPh)$_8$TPC] (TPC = *meso*-triphenylcorrole). The syntheses are convenient and apparently quite general; preliminary experiments indicate that other UPC derivatives, including the free-base ligands and various metal complexes, should also be accessible via an analogous strategy.

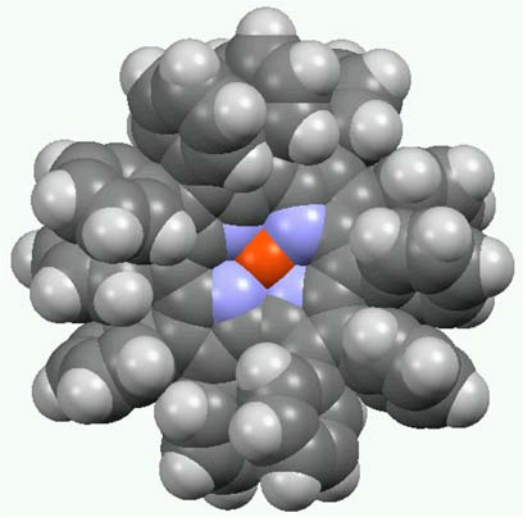

Figure 1. Space-filling model of Cu-UPC as a paradigm of a sterically hindered metallocorrole.

The copper complexes reported herein are of considerable interest in their own right. Uniquely among metallocorroles, which are generally planar (regardless of peripheral steric crowding),[6] copper corroles exhibit *inherent* saddling (even in the absence of a sterically hindered set of substituents). This saddling is primarily an electronic effect, a result of a copper ($d_{x^2-y^2}$)−corrole ("a_{2u}") orbital interaction (Figure 3),[9] but it is accentuated by sterically hindered substituents.[10,11] The molecular structure of a Cu-UPC derivative is thus of considerable interest, and we report here the first such X-ray structure. Electrochemical and electronic absorption studies on the new compounds also

Received: June 28, 2012
Published: September 6, 2012

   dx.doi.org/10.1021/ic301388e | *Inorg. Chem.* 2012, 51, 9911−9916

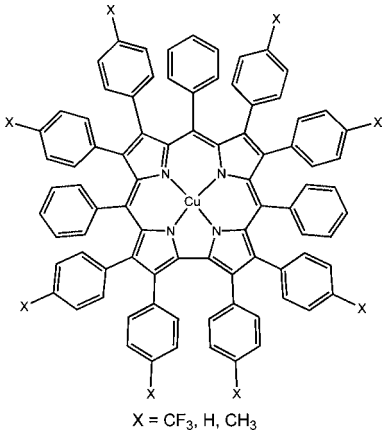

Figure 2. Cu[(4-XPh)$_8$TPC] derivatives reported in this study.

shed significant light on β-substituent effects on metallocorroles. Relatively little is known about the subject because, compared with *meso*-aryl substituents, β substituents on porphyrins and corroles are not as easily manipulated. To date, we have reported five different Cu-TPC series with varying β substituents, viz., Ph, H, Br,[12] F,[13] and CF_3.[14] A comparison of the five series affords unique insight into the interplay of electronic and steric effects on metallocorroles.

The new UPC derivatives were synthesized from Cu[Br$_8$TPC][12] and the appropriate arylboronic acid in refluxing toluene under anerobic conditions with $Pd_2(dba)_3{\cdot}CH_2Cl_2$ (dba = dibenzylidene acetone) as the catalyst. Except for the catalyst, these conditions are similar to those used in early syntheses of dodecaphenylporphyrins (DPPs) by Muzzi et al.[2a] The use of $Pd(PPh_3)_4$, the catalyst used by these authors, however, led to significantly longer reaction times. Aerobic conditions led to drastically lower yields. The reaction appeared to be faster with more electron-donating *p*-X groups on arylboronic acid, taking approximately 1.5, 2.0, and 2.5 days for X = CH_3, H, and CF_3, respectively (progress being monitored with electrospray ionization mass spectrometry). The yields, however, exhibited an opposite dependence on X: 41, 56, and 82% for CH_3, H, and CF_3, respectively.

RESULTS AND DISCUSSION

a. Molecular Structure of Cu[(4-CF$_3$Ph)$_8$TPC]·2C$_6$H$_{14}$. Small X-ray-quality crystals, with dimensions of 0.06 × 0.01 × 0.01 mm^3, were obtained for one of the complexes, Cu[(4-CF$_3$Ph)$_8$TPC], and the structure could be solved at the ALS, Berkeley, CA (Figure 4). The asymmetric unit consists of half of the corrole and one hexane molecule. The copper corrole is bisected by a crystallographic C_2 axis, aligned along the Cu−C$_{10}$ (meso) vector. The structure, including *all* of the CF_3 groups (somewhat remarkably), is fully ordered. The corroles stack upon each other along the *c* axis (space group *C*2/*c*). Their sterically hindered nature and helical shape, however, result in a pocket containing two hexane molecules, with an inversion-related corrole closing the pocket.

The copper corrole macrocycle exhibits a fairly strongly saddled conformation. The two symmetry-distinct saddling dihedrals C8−C9−C9′−C8′ and C3−C4−C6−C7 are 60.1 and 66.0°, respectively (see Figure 4). Qualitatively, the conformation resembles that of other copper corroles and of various DPP derivatives. The origin of the saddling, however, is very different for corroles, relative to porphyrins. For DPP derivatives,[15] the saddled geometries are a consequence of their sterically hindered nature. By contrast, steric hindrance is almost never sufficient for bringing about saddling in metallocorroles, as illustrated by several sterically hindered, undecasubstituted metallocorroles with planar macrocyclic cores (see ref 6c for a detailed discussion). As mentioned, copper corroles are an important exception in this regard in that they are inherently saddled on electronic grounds.[9] As shown in Figure 3, saddling allows some of the electron density of a corrole "a_{2u}-type" highest occupied molecular orbital (HOMO; using porphyrin nomenclature) to flow into the empty $d_{x^2-y^2}$ orbital of the formally trivalent metal center. The copper center is thus not true Cu^{III} but has significant Cu^{II} character. The degree of saddling observed for Cu[(4-CF$_3$Ph)$_8$TPC] is significantly higher than that observed for Cu-TPC derivatives and marginally smaller than what is found for Cu[Br$_8$TPC] derivatives.[6c,9,10] In other words, the β-aryl groups accentuate the saddling relative to β-H, but not quite as much as β-Br groups.

b. Electrochemistry. Figure 5 presents the cyclic voltammograms of the three Cu-UPC derivatives studied and Table 1 the corresponding redox potentials. Clearly, the para substituents on the β-aryl groups exercise a significant effect on both the oxidation and reduction potentials, which may be modeled by Hammett-type equations, as follows:[16]

$$E_{1/2ox1}/V = 0.35\sigma_p + 0.71$$

$$E_{1/2red1}/V = 0.49\sigma_p + 0.43$$

Recalling that there are eight β-aryl groups, the substituent effect per β-aryl group is given by

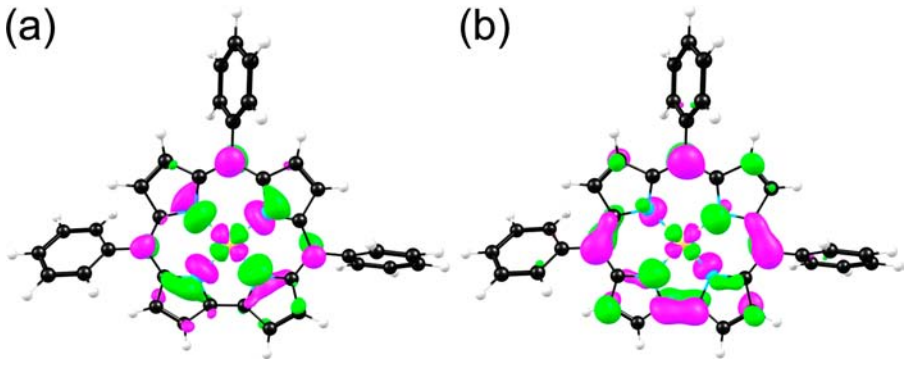

Figure 3. Frontier orbitals (OLYP/TZP) of Cu-TPC: (a) LUMO; (b) HOMO.

dx.doi.org/10.1021/ic301388e | *Inorg. Chem.* 2012, 51, 9911−9916

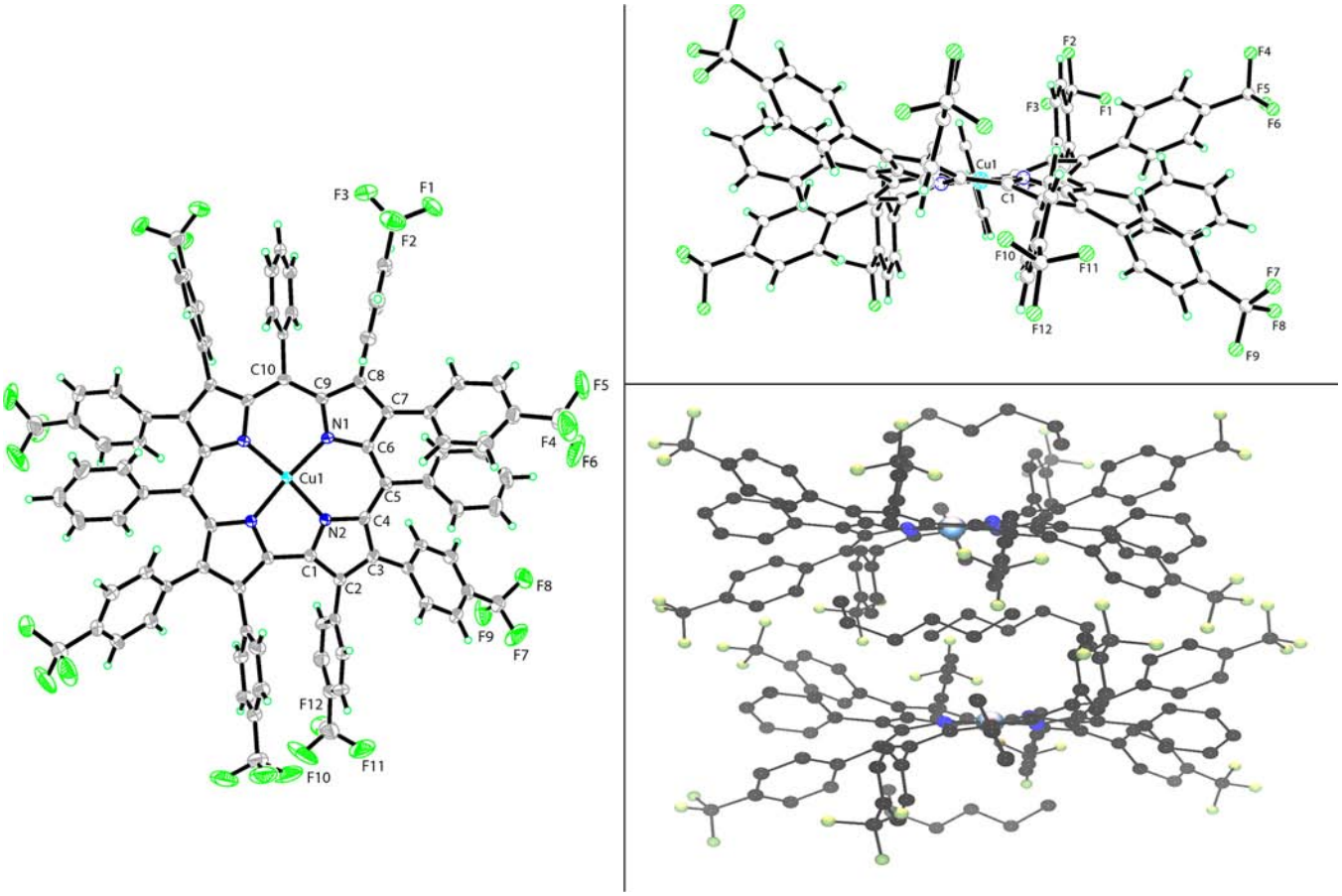

Figure 4. Left and top right: Thermal ellipsoid diagrams (two different views at the 50% probability level) for Cu[(4-CF_3Ph)$_8$TPC]. Bottom right: Stacking of two inversion-related corroles. The structures on the right side have been viewed along the *b* axis (parallel to the molecular C_2 axes). Distances (Å): Cu–N1 1.897, Cu–N2 1.902. Dihedrals (deg): C2–C1–C1–C2 40.9, C3–C4–C6–C7 60.1, C8–C9–C9′–C8′ 66.0, the primed atoms are the C_2-related counterparts of the corresponding unprimed atoms.

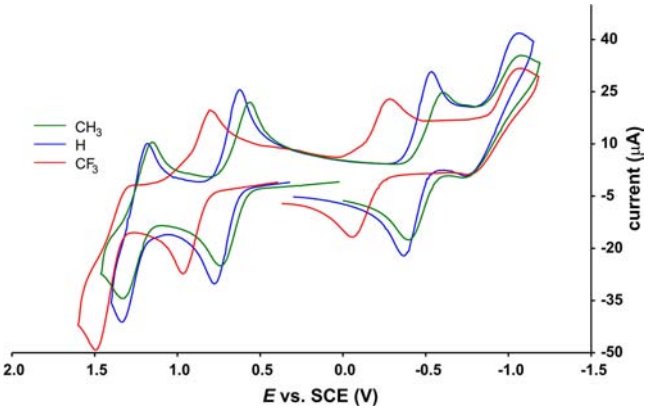

Figure 5. Cyclic voltammograms of Cu[(4-XPh)$_8$TPC] (X = CF_3, H, CH_3) in CH_2Cl_2.

Table 1. Cu-UPC Redox Potentials (V vs SCE) in CH_2Cl_2

complex	$E_{1/2ox1}$	$E_{1/2ox2}$	$E_{1/2red1}$	$E_{1/2red2}$
Cu[(4-CF_3Ph)$_8$TPC]	0.89	1.36	−0.17	−0.90
Cu-UPC	0.70	1.25	−0.45	−0.89
Cu[(4-CH_3Ph)$_8$TPC]	0.65	1.23	−0.50	−0.91

$$\frac{1}{8}\frac{dE_{1/2ox1}}{d\sigma} = \frac{0.35\ V}{8} = 44\ mV$$

$$\frac{1}{8}\frac{dE_{1/2red1}}{d\sigma} = \frac{0.49\ V}{8} = 61\ mV$$

For comparison, the effect of a para substituent in the *meso*-triarylcorrole series, Cu[T(4-XP)C], is given by[12]

$$\frac{1}{3}\frac{dE_{1/2ox1}}{d\sigma} = 32\ mV$$

$$\frac{1}{3}\frac{dE_{1/2red1}}{d\sigma} = 23\ mV$$

Para substituents on *β*-aryl groups thus are more effective at tuning the electronic character of the copper corrole core than para substituents on *meso*-aryl groups. This result is somewhat unexpected, given that both the HOMO and lowest unoccupied molecular orbital (LUMO) of copper corroles have large amplitudes at the meso positions but only small ones at the *β* positions. A plausible explanation is that the electronic effects of aryl substituents have a large through-space, electrostatic component.

In concert with our earlier contributions on metallocorroles,[16] this study affords some of the first detailed insights into *β*-substituent effects on copper corroles. The first oxidation and reduction potentials of the five Cu[X_8TPC] (X = Ph, H, Br, F, CF_3) derivatives are listed in Table 2, along with Hammett substituent constants,[17] Charton's steric parameters (ν_X),[17] and the corrole saddling dihedral (ω, defined as the C8–C9–C9′–C8′

dx.doi.org/10.1021/ic301388e | Inorg. Chem. 2012, 51, 9911–9916

Table 2. Redox Potentials of Cu[X_8TPC] (V vs SCE) as a Function of the β Substituents X

X	σ_p	σ_p^+	σ_p^-	$E_{1/2ox1}$	$E_{1/2red1}$	ν_X	ω (deg)
Ph	−0.01	−0.18	0.02	0.70	−0.45	1.66	66
H	0.00	0.00	0.00	0.76	−0.20	0.00	46[9]
Br	0.15	0.23	0.25	1.14	0.12	0.65	68[10]
F	0.06	−0.07	−0.03	1.15	0.22	0.27	na[a]
CF_3	0.53	n.a.	0.65	1.39	0.26	0.91	85[11]

[a]na = not available.

or C8−C9−C11−C12 torsion). Compared with the Cu[(4-XPh)$_8$TPC] derivatives discussed above, the complexes listed in Table 2 are more diverse, not only in terms of the electronic character of the β substituents but also in terms of their steric character, which leads to substantial differences in saddling across the five molecules. Overall, both $E_{1/2ox1}$ and $E_{1/2red1}$ vary over a wide range, nearly 700 mV. An interesting question concerns whether we can analyze and model the *interplay* of the substituent electronic effects and macrocycle distortion.

Not surprisingly, when steric effects and nonplanar distortions are ignored, the redox potentials exhibit poor-to-modest correlation with the Hammett σ_p constants of the β substituents (as reflected in R^2):

$$E_{1/2ox1}/V = 0.35\sigma_p + 0.71 \qquad R^2 = 0.71$$

$$E_{1/2red1}/V = 0.49\sigma_p - 0.43 \qquad R^2 = 0.44$$

Including the saddling dihedral as a variable in a bilinear analysis led to a good fit for oxidation potentials but less so for reduction potentials:[18]

$$E_{1/2ox1} = 1.167\sigma_p + 0.00090\omega + 0.7436 \qquad R^2 = 0.99$$

$$E_{1/2red1} = 1.482\sigma_p - 0.00752\omega + 0.1802 \qquad R^2 = 0.77$$

Using the Hammett constants σ_p^+ and σ_p^- did not result in significantly improved fits. Thus, we cannot yet offer a simple equation describing the redox potentials of Cu-TPC derivatives as a function of the β substituents X, especially when the electronic and steric character of X varies widely.

The electrochemical data (Tables 1 and 2) do, however, afford a rather clear comparison of the electronic character of the UPC ligands. Cu-UPC and Cu-TPC derivatives are oxidized with comparable ease, but the former are significantly more resistant to reduction. As sterically hindered catalysts for oxidative processes, therefore, metallo-UPC derivatives with electron-withdrawing β-aryl groups are likely to be more rugged and effective.

c. Electronic Absorption Spectra. The Soret maxima of various Cu-TPC derivatives shift sensitively as a function of the para substituents on *meso*-aryl groups (Table 3).[19] From X = CF_3 to CH_3, the Soret maximum of Cu[T(4-XP)C] red-shifts by 11 nm and that of Cu[Br_8T(4-XP)C] by 17 nm. According to time-dependent density functional theory (TDDFT) calculations, these shifts reflect aryl-to-Cu charge-transfer character in the Soret region. As shown in Figure 6, the corresponding shift for Cu[(4-XPh)$_8$TPC] is much smaller, only about 5 nm between X = CF_3/H and CH_3. Unfortunately, although TDDFT calculations have provided crucial qualitative insights into copper corrole spectra, they (as they are implemented to date) do a poor job of reproducing the Soret shifts.[19] At this point, therefore, we report these results simply as an interesting observation, without attempting to rationalize them.

Table 3. Comparison of *meso*- vs *p*-XPh β-Substituent Effects on Soret λ_{max} (nm)

	X =			
complex	CF_3	H	F	CH_3
Cu[(4-XPh)$_8$TPC]	441	441	443	445
Cu[T(4-XP)C]	407	413	412	418
Cu[Br_8T(4-XP)C]	436	439	445	453
Cu[(CF_3)$_8$T(4-XP)C]	na	459	462	471

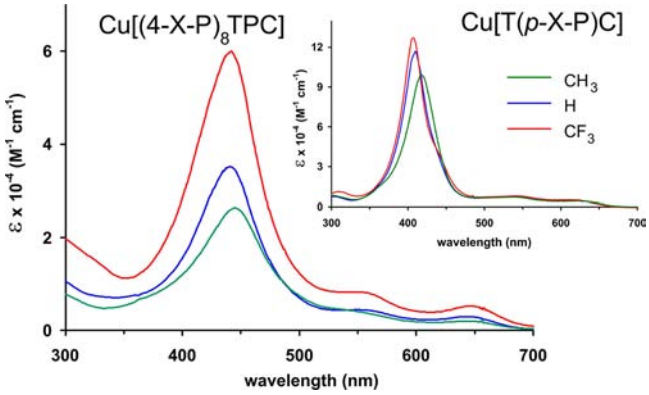

Figure 6. Electronic absorption spectra of Cu[(4-XPh)$_8$TPC] in CH_2Cl_2, with those of Cu[T(4-XP)C] also shown for comparison (top right).

The absolute values of the Soret maxima (in nm) of the Cu[(4-XPh)$_8$TPC] derivatives are roughly similar to those of Cu[Br_8T(4-XP)C] and significantly higher than those of Cu[T(4-XP)C]. The nonplanar distortion of the Cu[(4-XPh)$_8$TPC] series, however, is intermediate between that of Cu[T(4-XP)C] and that of the Cu[Br_8T(4-XP)C] series. The roughly 30-nm red shift of the Soret maxima of the Cu-UPC series relative to the Cu-TPC series thus appears to be attributable in part to a difference in macrocycle conformation and in part to β-aryl electronic effects, the latter suggesting that certain of the key molecular orbitals involved in Soret-region transitions have significant β-aryl character.

CONCLUSION

In summary, we have described a first major study of UPC derivatives, including the first crystal structure of such a species. Some of the key conclusions are: (a) The degree of saddling observed for Cu[(4-CF_3Ph)$_8$TPC] (60−66° within the dipyrromethane units) is higher than that observed for β-unsubstituted Cu-TPC derivatives (45−50°) but slightly lower than that for Cu[Br_8TPC] derivatives (70°). (b) The Soret maxima of the Cu-UPCs, interestingly, are similar to those of Cu[Br_8TPC] derivatives and are redshifted by some 30 nm relative to those of Cu-TPCs. (c) Para substituents on the β-phenyl groups tune the redox potentials of copper corroles more effectively than those on *meso*-phenyl substituents, while the opposite applies for Soret maxima.

The simple and effective syntheses described here open the door for much new, exciting work on UPC derivatives. Preliminary experiments indicate that both the free-base forms and other metal complexes of UPCs should be accessible via a Suzuki−Miyaura-based approach. Investigations into the reactivity and catalytic behavior of metallo-UPCs are then an obvious next step. Another line of inquiry concerns the dynamics of

dx.doi.org/10.1021/ic301388e | Inorg. Chem. 2012, 51, 9911−9916

Cu-UPC derivatives and of other sterically hindered copper corroles. Because of saddling, these are inherently chiral chromophores, which we have only synthesized in racemic form to date.[10,11,20] Detailed studies of the energetics and geometric pathway of the enantiomerization process are underway in our laboratory and will be reported in due course; isolation of the pure enantiomers and their characterization by various chiroptical methods are similarly other important goals.

EXPERIMENTAL SECTION

Materials. All reagents and solvents were used as purchased. Toluene was predried by distillation from CaH_2 and then distilled from sodium-benzophenone. Silica gel 60 (0.04−0.063 mm particle size; 230−400 mesh, Merck) was used for flash chromatography. Silica gel 60 preparative thin-layer chromatographic plates (20 × 20 cm; 0.5 mm thick, Merck) were used for the final purification of the new complexes. The starting material Cu[Br_8TPC] was synthesied as previously reported.[12]

Instrumentation. Ultraviolet−visible (UV−vis) spectra were recorded on an HP 8453 spectrophotometer. Cyclic voltammetry was performed with an EG&G model 263A potentiostat having a three-electrode system: a glassy carbon working electrode, a platinum wire counter electrode, and a saturated calomel reference electrode (SCE). Tetra(*n*-butyl)ammonium perchlorate, recrystallized twice from absolute ethanol and dried in a desiccator for at least 2 weeks, was used as the supporting electrolyte. The reference electrode was separated from the bulk solution by a fritted-glass bridge filled with a solvent/supporting electrolyte mixture. All potentials were referenced to the SCE. The anhydrous dichloromethane solutions were purged with argon for at least 5 min prior to measurements. An argon blanket was maintained over the solutions during the electrochemical measurements. ^{1}H NMR spectra (600 MHz) were recorded in CD_2Cl_2 (referenced to 5.30 ppm) at 298 K on a Varian Inova spectrometer equipped with a cryogenically cooled inverse triple-resonance probe. ^{19}F NMR spectra (376 MHz) were acquired at 298 K and referenced to 2,2,2-trifluoroethanol-d_3 (δ = −77.8 ppm) on a Mercury Plus Varian spectrometer. High-resolution electrospray ionization (HR-ESI) mass spectra were recorded on an LTQ Orbitrap XL spectrometer.

General Procedure for the Synthesis of Undecaarylcorroles. Cu[Br_8TPC] (20 mg), arylboronic acid (40 equiv), potassium carbonate (40 equiv), and $Pd_2(dba)_3$·$CHCl_3$ (0.1 equiv) were introduced into a 50-mL three-necked, round-bottomed flask fitted with a reflux condenser and a magnetic stirring bar. The reaction setup was degassed with argon, followed by the addition of dry toluene (10 mL). The suspension was purged with argon for 10 min and stirred at 100−105 °C under argon for 1.5−2.5 days. Progress of the reaction was monitored by mass spectrometry. After complete consumption of octabromocorrole, the product mixture was cooled to room temperature, diluted with 10 mL of CH_2Cl_2, and washed with saturated aqueous $NaHCO_3$ and then with distilled water. The CH_2Cl_2 phase was dried with anhydrous Na_2SO_4, filtered, and evaporated. The brown residue obtained was purified by silica gel column chromatography with an *n*-hexane/CH_2Cl_2 mixture as the eluent. The product eluted as an intense brown band, which was collected and evaporated to dryness. The residue obtained was purified by preparative thin-layer chromatography (PLC), as detailed below for each corrole. Spectroscopic data are also fully indicated, except for certain ^{HH}J's, which could not be discerned because of overlapping peaks.[20]

Copper 2,3,7,8,12,13,17,18-Octakis[4-(trifluoromethyl)-phenyl]-5,10,15-triphenylcorrole, Cu[(4-CF_3Ph)$_8$TPC]. The reaction was complete after 2.5 days (62 h). The brown residue obtained after workup was chromatographed on a silica gel column (14 × 3 cm) with 3:1 *n*-hexane/CH_2Cl_2 as the eluent. The complex was collected as the first brown band that faded into yellow after eluting with 0.8 L of the eluent. The corrole residue was further purified by PLC with 4:1 *n*-hexane/CH_2Cl_2. The last brown band was pure Cu[(4-CF_3Ph)$_8$TPC] (23.5 mg, 82%). The complex was crystallized as tiny brownish needles over 1 week by diffusion of CH_3OH into a CH_2Cl_2 solution. UV−vis (CH_2Cl_2): λ_{max}, nm ($\varepsilon \times 10^{-4}$, M^{-1} cm^{-1}): 442 (6.00), 546 (0.83), 646 (0.52). ^{1}H NMR (CD_2Cl_2): δ 7.08 (d, ^2J = 8.4 Hz, 4H, 2,18-*m*, CF_3Ph), 6.99 (d, ^2J = 8.4 Hz, 4H, 2,18-*o*, CF_3Ph), 6.97 (dd, ^2J = 8.4 Hz, ^3J = 1.2 Hz, 2H, 10-*o*, Ph), 6.94 (d, ^2J = 7.8 Hz, 4H, 3,17-*m*, CF_3Ph), 6.89 (d, ^2J = 8.4 Hz, 4H, 7,13-*m*, CF_3Ph), 6.85−6.83 (m, 4H, 5,15-*o*, Ph, 4H, 8,12-*m*, CF_3Ph), 6.80 (d, ^2J = 7.8 Hz, 4H, 3,17-*o*, CF_3Ph), 6.73 (tt, ^2J = 7.8 Hz, ^3J = 1.2 Hz, 2H, 5,15-*p*, Ph), 6.67−6.62 (m, 1H, 10-*p*, Ph, 8H, 7, 8,12,13-*o*, CF_3Ph), 6.46 (t, ^2J = 7.8 Hz, 4H, 5,15-*m*, Ph), 6.42 (t, ^2J = 7.8 Hz, 2H, 10-*m*, Ph).^{19}F NMR: δ −63.29 (bs, 6F), −63.33 (bs, 6F), −63.45 to −63.42 (overlapping bs, 12F). MS (HR-ESI major isotopomer): M^+ = 1739.27 (expt), 1739.27 (calcd). Elem anal. Found (calcd): C, 64.35 (64.20); H, 2.91 (2.72); N, 3.16 (3.22).

Copper 2,3,5,7,8,10,12,13,15,17,18-Undecaphenylcorrole, Cu-UPC. The reaction was complete after 2 days (49 h). The residue was passed through a silica gel column (14 × 3 cm) with 3:1 *n*-hexane/CH_2Cl_2. The first two bands (brown and yellow) were impurities. The next dark-brown band was the desired product and was eluted with 0.8 L of the eluent. The yellow impurity band that followed was discarded. The product was further purified by PLC with 3:1 *n*-hexane/CH_2Cl_2, where pure Cu[UPC] appeared as the last brown band (11.1 mg, 56%). UV−vis (CH_2Cl_2): λ_{max}, nm ($\varepsilon \times 10^{-4}$, M^{-1} cm^{-1}): 441 (3.51), 548 (0.44), 643 (0.29). ^{1}H NMR (CD_2Cl_2): δ 7.06 (dd, ^2J = 8.4 Hz, ^3J = 1.2 Hz, 2H, 10-*o*, Ph), 6.92 (dd, ^2J = 8.4 Hz, ^3J = 1.2 Hz, 4H, 5,15-*o*, Ph), 6.86−6.82 (m, 6H, 2,18-*m* and -*p*, Ph), 6.80−6.77 (m, 4H, 2,18-*o*, Ph), 6.69−6.52 (m, 10H, 3,17-*o*, -*m*, and -*p*; 2H, 5,15-*p*; 10H, 7,13-*o*, -*m*, and -*p*; 1H,10-*p*; 10H, 8,12-*o*, -*m*, and -*p*, Ph), 6.46−6.40 (m, 6H, 5,10,15-*m*, Ph). MS (HR-ESI major isotopomer): M^+ = 1194.37 (expt), 1194.37 (calcd). Elem anal. Found (calcd): C, 85.59 (85.37); H, 4.80 (4.64); N, 4.45 (4.68).

Copper 2,3,7,8,12,13,17,18-Octakis(4-methylphenyl)-5,10,15-triphenylcorrole, Cu[(4-CH_3Ph)$_8$TPC]. The reaction was complete after 1.5 days (39 h). After workup, the brown residue obtained was chromatographed on a silica gel column (14 × 3 cm) with 3:1 *n*-hexane/CH_2Cl_2 as the eluent. The first brown band was an impurity, but the next brown band was the desired complex. It gradually faded out to yellow and was completely eluted with 1.1 L of the eluent. A red impurity band followed thereafter and was discarded. The product was purified by PLC with 4:1 *n*-hexane/CH_2Cl_2. The last brown band was pure Cu[(4-CH_3Ph)$_8$TPC] (8.8 mg, 41%). UV−vis (CH_2Cl_2): λ_{max}, nm ($\varepsilon \times 10^{-4}$, M^{-1} cm^{-1}): 445 (2.64), 644 (0.20). ^{1}H NMR (CD_2Cl_2): δ 6.98 (dd, ^2J = 7.8 Hz, ^3J = 1.2 Hz, 2H, 10-*o*, Ph), 6.83 (d, ^2J = 7.2 Hz, 4H, 5,15-*o*, Ph), 6.73 (d, ^2J = 7.8 Hz, 4H, 2,18-*o*, tolyl), 6.68 (tt, ^2J = 7.2 Hz, ^3J = 1.2 Hz, 2H, 5,15-*p*, Ph), 6.63 (tt, ^2J = 7.8 Hz, ^3J = 1.2 Hz, 1H, 10-*p*, Ph), 6.59 (d, ^{2}-J = 7.8 Hz, 4H, 2,18-*m*, tolyl), 6.56 (d, ^2J = 7.2 Hz, 4H, 3,17*o*, tolyl), 6.47−6.36 (m, 8H, 7, 8, 12,13-*o*, tolyl; 12H, 3,7,8,12,13,17-*m*, tolyl, 6H, 5,10,15-*m*, Ph), 2.14 (s, 6H, 2,18-*p*-CH_3, tolyl), 2.01 (s, 6H, 3,17-*p*-CH_3, tolyl), 1.98 (s, 6H, 7,13-*p*-CH_3, tolyl) 1.94 (s, 6H, 8, 12-*p*-CH_3, tolyl). MS (HR-ESI, major isotopomer): M^+ = 1307.49 (expt), 1307.50 (calcd). Elem anal. Found (calcd): C, 85.53 (85.39); H, 5.67 (5.47); N, 4.19 (4.28).

X-ray Structure Determination of Cu[(4-CF_3Ph)$_8$TPC]·2C_6H_{14}. A dichroic red-blue needle of dimensions 0.06 × 0.01 × 0.01 mm^3 was mounted in the 100(2)-K nitrogen cold stream provided by an Oxford Cryostream low-temperature apparatus on the goniometer head of a Bruker D85 diffractometer equipped with an Apex II CCD detector on Beamline 11.3.1 at the ALS, Berkeley, CA. Diffraction data were collected using synchrotron radiation monochromated with silicon(111) to a wavelength of 0.8856(1) Å. A full sphere of data, to 2θ = 63°, was collected using 0.3° ω scans. A multiscan absorption correction was applied using the program *SADABS 2008/1*. The data consist of 36315 reflections collected, of which 7223 were unique [R(int) = 0.0645] and 4843 were observed [$I > 2\sigma(I)$]. The space group was determined and the structure was solved by direct methods (*SHELXT*) and refined by full-matrix least squares on F^2 (*SHELXL-97*) using 608 parameters and zero restraints. The asymmetric unit contains half of the copper corrole and one hexane molecule. The whole corrole is generated by a 2-fold axis. The hydrogen atoms on the carbon atoms were generated geometrically and refined as riding atoms with C−H = 0.95−0.99 Å, U_{iso}(H) = 1.2U_{eq}(C) for aromatic carbon atoms and U_{iso}(H) = 1.5U_{eq}(C) for CH_3 groups. The maximum and minimum peaks in the final difference Fourier map were +1.023 and −0.563 e $Å^{-3}$.

dx.doi.org/10.1021/ic301388e | *Inorg. Chem.* 2012, 51, 9911−9916

Crystal data: $C_{105}H_{75}F_{24}N_4Cu$, M_w = 1912.23, monoclinic, $C2/c$, a = 25.4620(13) Å, b = 25.8918(12) Å, c = 16.2468(9) Å, β = 128.316(3)°, V = 8403.7(7) Å^3, T = 100(2) K, Z = 4, R1 [$I > 2\sigma(I)$] = 0.0550, wR2 (all data) = 0.1592, GOF (on F^2) = 1.039.

■ ASSOCIATED CONTENT

Supporting Information

Details of the synthesis and characterization, including X-ray analysis. This material is available free of charge via the Internet at http://pubs.acs.org.

■ AUTHOR INFORMATION

Corresponding Author

*E-mail: abhik.ghosh@uit.no.

Notes

The authors declare no competing financial interest.

■ ACKNOWLEDGMENTS

This work was supported by the Research Council of Norway and the ALS, LBNL. We thank Drs. Arnfinn Kvarsnes and Johan Isaksson for assistance with the NMR measurements and Dr. Jeanet Conradie for assistance with graphics and data analysis.

■ REFERENCES

(1) Reviews on sterically hindered and/or nonplanar porphyrins: (a) Shelnutt, J. A.; Song, X.-Z.; Ma, J.-G.; Jia, S. L.; Jentzen, W.; Medforth, C. J. *Chem. Soc. Rev.* **1998**, *27*, 31−42. (b) Senge, M. *Chem. Commun.* **2006**, 243−256.

(2) Early syntheses of DPPs: (a) Muzzi, C. M.; Medforth, C. J.; Voss, L.; Cancilla, M.; Lebrilla, C.; Ma, J. G.; Shelnutt, J. A.; Smith, K. M. *J. Tetrahedron Lett.* **1999**, *40*, 1−5. (b) Zhou, X.; Tse, M. K.; Wan, T. S.; Chan, K. S. *J. Org. Chem.* **1996**, *61*, 3590−3593.

(3) Bhyrappa, P.; Young, J. K.; Moore, J. S.; Suslick, K. S. *J. Mol. Catal. A* **1996**, *113*, 109−116.

(4) For a report on mono- and binuclear ruthenium corroles, see: Simkhovich, L.; Luobeznova, I.; Goldberg, I.; Gross, Z. *Chem.—Eur. J.* **2003**, *9*, 201−208.

(5) Metal-metal−bonded porphyrin dimers: Collman, J. P.; Arnold, J. P. *Acc. Chem. Res.* **1993**, *26*, 586−592.

(6) (a) Aviv-Harel, I.; Gross, Z. *Chem.—Eur. J.* **2009**, *15*, 8382−8394. (b) Palmer, J. H. *Struct. Bonding (Berlin)* **2011**, *142*, 49−90. (c) Thomas, K. E.; Alemayehu, A. B.; Conradie, J.; Beavers, C. M.; Ghosh, A. *Acc. Chem. Res.* **2012**, *45*, 1203−1214.

(7) Scrivanti, A.; Beghetto, V.; Matteoli, U.; Antonaroli, S.; Marini, A.; Mandoj, F.; Paolesse, R.; Crociani, B. *J. Tetrahedron Lett.* **2004**, *45*, 5861−5864.

(8) Suzuki, A. *Angew. Chem., Int. Ed.* **2011**, *50*, 6722−6737.

(9) Inherent, electronically driven saddling was first recognized in: Alemayehu, A. B.; Gonzalez, E.; Hansen, L. K.; Ghosh, A. *Inorg. Chem.* **2009**, *48*, 7794−7799.

(10) Alemayehu, A. B.; Gonzalez, E.; Ghosh, A. *Inorg. Chem.* **2010**, *49*, 7608−7610.

(11) Thomas, K. E.; Conradie, J.; Hansen, L. K.; Ghosh, A. *Eur. J. Inorg. Chem.* **2011**, 1865−1870.

(12) Wasbotten, I. H.; Wondimagen, T.; Ghosh, A. *J. Am. Chem. Soc.* **2002**, *124*, 8104−8116.

(13) Steene, E.; Dey, A.; Ghosh, A. *J. Am. Chem. Soc.* **2003**, *125*, 16300−16309.

(14) Thomas, K. E.; Wasbotten, I. H.; Ghosh, A. *Inorg. Chem.* **2008**, *47*, 10469−10478. Addition/correction: *Inorg. Chem.* **2009**, *48*, 1257−1257.

(15) (a) Nurco, D. J.; Medford, C. J.; Forsyth, T. P.; Olmstead, M. M.; Smith, K. M. *J. Am. Chem. Soc.* **1996**, *118*, 10918−10919. (b) Nurco, D. J.; Medforth, C. J.; Forsyth, T. P.; Olmstead, M. M.; Smith, K. M. *J. Am. Chem. Soc.* **1992**, *114*, 9859−9869. (c) Yokoyama, A.; Kojima, T.; Ohkubo, K.; Fukuzumi, S. *Inorg. Chem.* **2010**, *49*, 11190−11198.

(16) Substituent effects on copper corroles have been examined electrochemically in a number of papers from our laboratory[12−14] but most notably in: Ou, Z.; Shao, J.; Zhao, H.; Ohkubo, K.; Wasbotten, I. H.; Fukuzumi, S.; Ghosh, A.; Kadish, K. M. *J. Porphyrins Phthalocyanines* **2004**, *8*, 1236−1247.

(17) Williams, A. *Free Energy Relationships in Organic and Bioorganic Chemistry*; Royal Society of London: London, 2003; pp 1−297.

(18) We have preferred to use the saddling dihedral over Charton's ν_X parameter because the latter, essentially a radius most appropriate for three-dimensional groups, is not particularly meaningful for planar β-aryl substituents. The steric effects of the β-aryl groups are far lower than that implied by the very high ν_X value shown in Table 2.

(19) Substituent effects on the electronic absorption spectra of copper corroles have been examined in a number of papers from our laboratory[12−14] but most notably in: (a) Alemayehu, A. B.; Conradie, J.; Ghosh, A. *Eur. J. Inorg. Chem.* **2011**, *12*, 1857−1864. (b) Alemayehu, A. B.; Conradie, M. M.; Ghosh, A. *J. Porphyr. Phthalocya.* **2012**, *16*, 695−704.

(20) The temperature-dependent NMR dynamics of the Cu-UPC derivatives is of significant interest. At room temperature, the ortho or meta protons on each aryl group are equivalent, as a result of phenyl rotation.[2a] DFT calculations suggest that enantiomerization via saddling inversion entails a rather high activation barrier. A full exposition of these results will follow shortly in a separate paper on the subject.